Nutrition Research and Practice 2020;14(1):3-11

http://e-nrp.org

Neuroprotective effects of urolithin A on H_2O_2-induced oxidative stress-mediated apoptosis in SK-N-MC cells

Kkot Byeol Kim[1], Seonah Lee[1] and Jung Hee Kim[1,2§]

[1]Research Institute, Seoul Medical Center, Seoul 02053, Korea
[2]Department of Neurosurgery, Seoul Medical Center, 156 Shinnea-ro, Seoul 02053, Korea

BACKGROUND/OBJECTIVES: Oxidative stress causes cell damage and death, which contribute to the pathogenesis of neurodegenerative diseases. Urolithin A (UA), a gut microbial-derived metabolite of ellagitannins and ellagic acid, has high bioavailability and various health benefits such as antioxidant and anti-inflammatory effects. However, it is unknown whether it has protective effects against oxidative stress-induced cell death. We investigated whether UA ameliorates H_2O_2-induced neuronal cell death.
MATERIALS/METHODS: We induced oxidative damage with 300 μM H_2O_2 after UA pretreatment at concentrations of 1.25, 2.5, and 5 μM in SK-N-MC cells. Cytotoxicity and cell viability were determined using the CCK-8 assay. The formation of reactive oxygen species (ROS) was measured using a 2,7-dichlorofluorescein diacetate assay. Hoechst 33342 staining was used to characterize morphological changes in apoptotic cells. The expressions of apoptosis proteins were measured using Western blotting.
RESULTS: UA significantly increased cell viability and decreased intracellular ROS production in a dose-dependent manner in SK-N-MC cells. It also decreased the Bax/Bcl-2 ratio and the expressions of cytochrome c, cleaved caspase-9, cleaved caspase-3, and cleaved PARP. In addition, it suppressed the phosphorylation of the p38 mitogen-activated protein kinase (MAPK) pathway.
CONCLUSIONS: UA attenuates oxidative stress-induced apoptosis via inhibiting the mitochondrial-related apoptosis pathway and modulating the p38 MAPK pathway, suggesting that it may be an effective neuroprotective agent.

Nutrition Research and Practice 2020;14(1):3-11; https://doi.org/10.4162/nrp.2020.14.1.3; pISSN 1976-1457 eISSN 2005-6168

Keywords: Neurodegenerative diseases, metabolite, reactive oxygen species, apoptosis, p38MAPK

INTRODUCTION

Oxidative stress is involved in the pathogenesis of diseases such as cardiovascular disease, chronic kidney disease, neurodegenerative diseases (NDs), macular degeneration, and cancer [1]. Reactive oxygen species (ROS) generated during normal metabolic processes of cells are removed by intracellular antioxidant enzymes, but imbalances between the production and elimination of ROS that result from abnormalities of the antioxidant homeostasis system induce oxidative stress [2-4]. Oxidative stress causes peroxidation of lipids in the cell membrane, impairment of intracellular essential components such as proteins and DNA, induction of mitochondrial dysfunctions, and activation of apoptosis-related cell signals, eventually leading to fatal injury and cell death [5,6].

NDs including Alzheimer's disease (AD) and Parkinson's disease (PD) lead to progressive loss of cognitive and behavioral capacities, resulting in severe disability and death [7]. Although pathological mechanisms involving NDs are complex and have not yet been fully elucidated [6], apoptosis induced by oxidative stress and abnormal protein aggregation are major causes of pathogenesis [7-9]. Thus, protecting neuronal cells from injury by oxidative stress is considered a promising therapeutic approach for the treatment of NDs in terms delaying progression and improving status of disease [10].

According to epidemiological studies and many *in vitro* and *in vivo* intervention studies, dietary polyphenols have many health benefits such as antioxidant, anti-inflammatory, anticancer, anti-obesity, anti-diabetic, and neuroprotective effects [3]. However, because only 5-10% of dietary polyphenols are absorbed in the small intestine, to apply as dietary agents for the prevention or treatment of diseases has the limitation [11,12]. Several studies have recently reported that the health benefits of polyphenol-rich foods are mainly due to their gut microbial-derived metabolites, not their polyphenol compounds [12,13]. Polyphenols are converted into phenolic metabolites of small molecular weight by the action of gut microbiota in the small intestine; these gut microbial-derived metabolites have high bioavailability and permeability of the blood-brain barrier (BBB) [14].

Ellagitannins (ETs) are hydrolyzed into ellagic acid (EA) in the body after ingestion of polyphenols in pomegranates, walnuts,

This study was supported by grants from the Seoul Medical Center Research Institute, Republic of Korea (Grant #18-C20).
§ Corresponding Author: Jung Hee Kim, Tel. 82-2-2276-8601, Fax. 82-2-2276-7435, Email. nostoi72@naver.com
Received: June 27, 2019, Revised: July 11, 2019, Accepted: September 6, 2019

and berries. ETs and EA have excellent antioxidant and cell-protective abilities but they are also limited in having low bioavailabilities; thus, studies have increasingly investigated gut microbial-derived metabolites such as urolithins (uros) [15,16]. Uros have been found in various forms such as Uro-M5, Uro-M6, Uro-M7, Uro-D, Uro-C, Uro-B, Uro-A, and isoUro-A. Among them, Uro-A (UA) is the most common form in humans. It has health benefits such as antioxidant, anti-cancer, anti-inflammation, and anti-obesity effects *in vivo* and *in vitro* [17,18]. However, there have been no reports on the effects of UA on brain-related diseases, such as NDs caused by oxidative stress.

In this study, we investigated the protective effects of UA against H_2O_2-induced oxidative stress in human neuroblastoma SK-N-MC cells. We also examined possible mechanisms associated with the action of UA.

MATERIALS AND METHODS

Materials

The SK-N-MC human neuroblastoma cell line was purchased from American Type Culture Collection (Rockville, MD, USA). Eagle's minimum essential medium (EMEM), trypsin-EDTA, antibiotics, Dulbecco's phosphate-buffered saline (PBS), and Hank's balanced salt solution (HBSS) were purchased from WelGENE (Daegu, Republic of Korea). Fetal bovine serum (FBS), urolithin A (UA), and general reagents were purchased from Sigma-Aldrich (St. Louis, MO, USA). Cell counting Kit-8 (CCK-8) assay reagents were purchased from Dojindo Molecular Technologies (Gaithersburg, MD, USA), and the intracellular ROS assay kit was purchased from Cell Biolabs (San Diego, CA, USA). Anti-Bax (#2772), anti-total p38 (#9212), anti-caspase-9 (#9502), anti-caspase-3 (#9665), anti-PARP (poly (ADP-ribose) polymerase, #9532), anti-mouse IgG horseradish peroxidase [HRP]-conjugated antibody (#7076), anti-rabbit IgG HRP-conjugated antibody (#7074), and p38 mitogen-activated protein kinase (MAPK) inhibitor SB203580 (#5633) were purchased from Cell Signaling Technology (Danvers, MA, USA).

Cell culture and treatment

SK-N-MC cells were grown in EMEM supplemented with 10% FBS and 1% antibiotics, and maintained in a humidified incubator at 37°C in an atmosphere of 5% CO_2 and 95% air. The cell culture medium was changed every 2 days. When the cells were approximately 90% confluent, they were subcultured in plates at an appropriate density according to each experimental scale. The cells were pretreated with various concentrations (1.25, 2.5, and 5 μM) of UA for 6 h and then exposed to 300 μM H_2O_2 for 18 h.

Measurement of cell viability

The cell viability was evaluated using a CCK-8 assay [19]. CCK-8 is reduced by dehydrogenases in cells to give a yellow-colored product (formazan). The amount of the formazan dye generated by the activity of dehydrogenases in cells is directly proportional to the number of living cells. This characteristic can be used for cell viability analysis. The cells were seeded at 5×10^4 cells/100 μL in a 96-well plate and cultured for 24 h to confirm cell viability. After the cultured cells had been treated with various concentrations of UA and H_2O_2 for various times, they were incubated with the CCK-8 solution for 2 h. Then absorbance at 450 nm was measured using a microplate reader (Sunrise; Tecan, Grödig, Austria).

Measurement of intracellular ROS production

To measure the amount of ROS produced in cells, used the cell-permeable fluorogenic probe 2′, 7′-Dichlorodihydrofluorescin diacetate (DCFH-DA). In brief, DCFH-DA is diffused into cells and is deacetylated by cellular esterases to non fluorescent DCFH, which is rapidly oxidized to highly fluorescent DCF by ROS [20]. The cells were seeded at 8×10^4 cells/100 μL in a 96-well black plate. After 24 h, the cells were treated with 1.25, 2.5, and 5 μM UA and cultured for 6 h. The cell culture medium was removed and the cells were washed twice with HBSS, treated with 10 μM DCFH-DA solution, and incubated for 45 min. The DCFH-DA solution was removed and the cells were washed twice with HBSS and then treated with 300 μM H_2O_2. Intracellular fluorescence intensities were measured at 485 nm and 530 nm using a fluorescence microplate reader (Infinite M200; Tecan).

Hoechst 33342 staining

Hoechst 33342 (Invitrogen, Carlsbad, CA, USA) staining was used to observe changes in the nuclei of apoptotic cells [21]. The cells were seeded at 4×10^5 cells/mL in a six-well plate, cultured for 2 days, then treated with various UA concentrations for 6 h. The medium containing UA was removed and the cells were cultured for 18 h in the presence of 300 μM H_2O_2. Then the cells were washed with PBS and fixed with 4% paraformaldehyde (Sigma-Aldrich) for 10 min at room temperature. After washing with PBS, Hoechst 33342 dye was used at a concentration of 5 μg/mL for 10 min to stain the cells. After staining and washing with PBS, the cells were observed using fluorescence microscopy (IX81; Olympus, Tokyo, Japan).

Western blotting analyses

After removing the culture medium from the treated cells, the cells were washed with PBS, and the proteins were extracted using an EzRIPA lysis kit (ATTO, Tokyo, Japan). Protein concentrations were quantified using the BCA method (Thermo Scientific, Rockford, IL, USA) and then the cells were mixed with 5× SDS sample buffer, followed by loading of 15 μg protein per sample well. The proteins were separated by electrophoresis on a 10-15% SDS-PAGE gel and transferred to a PVDF membrane (Merck Millipore, Darmstadt, Germany). After transfer, the membrane was blocked for 1 h with 5% skim milk (Sigma-Aldrich) in TBS-T buffer. Then the membranes were incubated with primary antibodies diluted at a ratio of 1:1,000, overnight at 4°C. After washing three times, HRP-conjugated secondary antibodies diluted 1:2,000 were added and allowed to react at room temperature for 1 h. After washing three times with TBS-T, protein bands were visualized after treatment with ECL-Western Blotting Substrate (Thermo Scientific).

Statistical analyses

The results are expressed as means ± SD. Statistical analyses included *t*-tests and one-way analysis of variance (ANOVA) using

SPSS statistical software for Windows, version 20.0 (SPSS, Chicago, IL, USA). A one-way ANOVA followed by Duncan's multiple range test was used to determine differences among the treatment groups. The test results were considered statistically significant at $P < 0.05$.

RESULTS

Effect of UA on cell viability

Human neuroblastoma SK-N-MC cells have been widely used as an *in vitro* model to study the pathogenesis of NDs such as AD because of their high stability and homogeneity [22,23]. The cell viabilities were determined using the CCK-8 assay. Cell viability was not significantly affected at UA concentrations up to 10 μM (Fig. 1B). We subsequently chose a UA concentration range of 0.1-10 μM that did not induce cytotoxicity in SK-N-MC cells. H_2O_2 significantly decreased cell viability in a dose-dependent manner; 300 μM indicated 63.1 ± 1.5% cell viability (Fig. 1C). To assess the neuroprotective effects of UA against H_2O_2, the cells were pretreated with UA for 6 h and then treated with 300 μM H_2O_2 for 18 h (Fig. 1D). Pretreatment with UA significantly increased cell viability compared to H_2O_2 alone (62.3 ± 1.3%). Pretreatment with different concentrations of UA (1.25, 2.5, and 5 μM) increased the cell viability to 70.2 ± 2.0, 76.9 ± 2.0, and 80.2 ± 4.0%, respectively. These results were also confirmed by observing cell morphologies (Fig. 1E).

Effects of UA on intracellular ROS production

To confirm that UA inhibited ROS production induced by H_2O_2, ROS levels in the cells were detected using DCFH-DA. Intracellular ROS production was increased by 2.34 ± 6.69-fold in the group treated with 300 μM H_2O_2, compared to the controls.

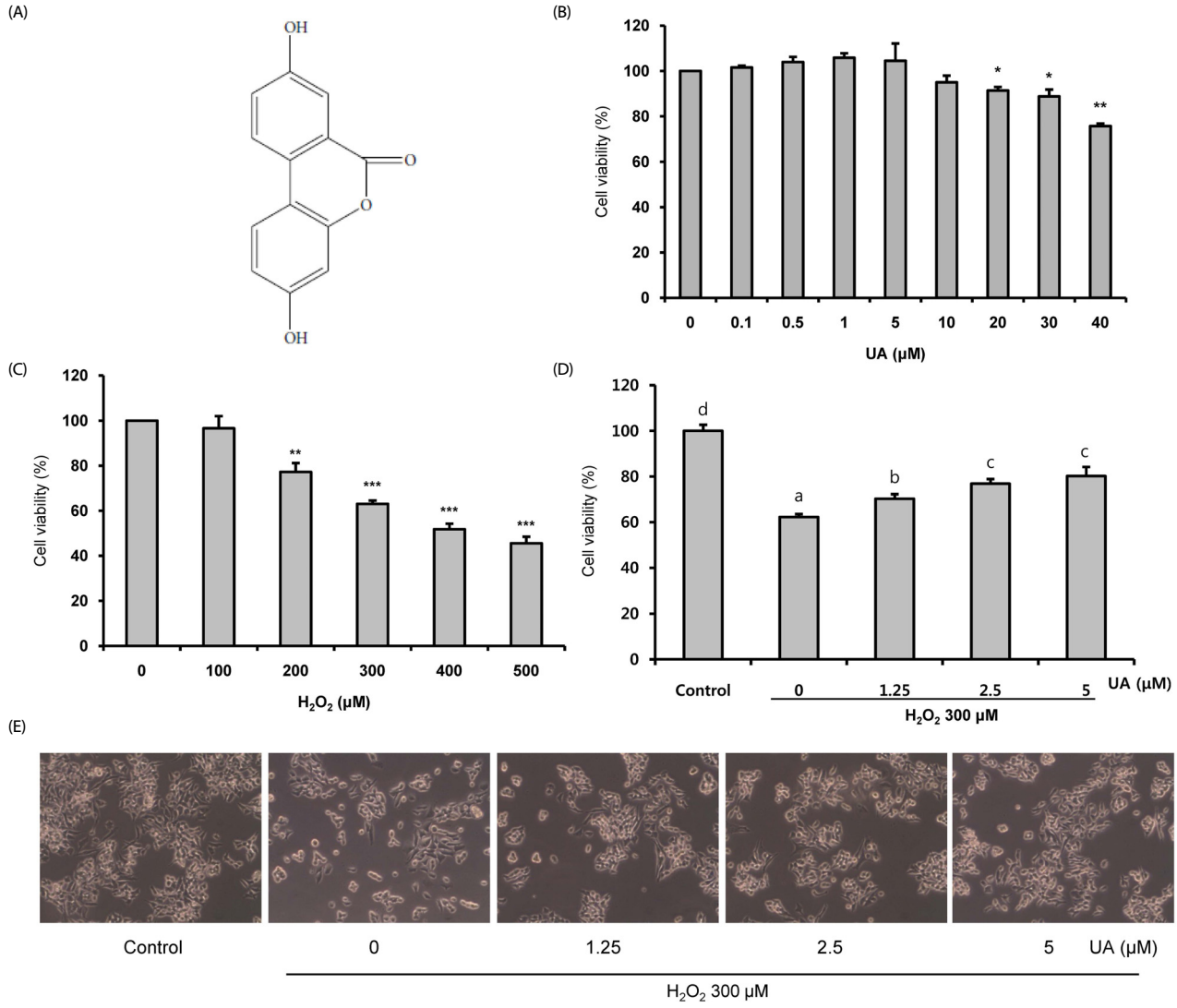

Fig. 1. Protective effects of urolithin A (UA) on H_2O_2-induced cell death and cytotoxicity in SK-N-MC cells. Cell viability was determined by CCK-8 assay. (A) The molecular of UA. (B) SK-N-MC cell were treated with increasing concentrations (0.1-40 μM) of UA for 24 h. (C) SK-N-MC cell were treated with increasing concentrations (100-500 μM) of H_2O_2 for 24 h. (D) The cell pretreated with UA at the indicated concentration (1.25-5 μM) for 6 h, and then treated with 300 μM H_2O_2 for 18 h. (E) The morphological change of SK-N-MC cells was observed using a microscope (magnification 100x). The results are expressed as mean ± SD. * $P < 0.05$, ** $P < 0.01$, *** $P < 0.001$ compared with control cells. Different letters indicate a significant difference according to analysis of variance ($P < 0.05$).

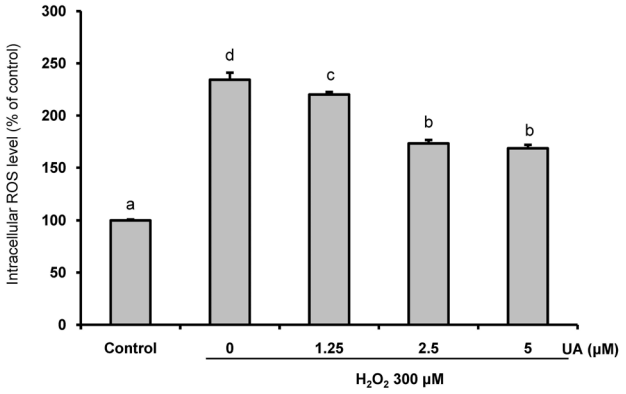

Fig. 2. Intracellular reactive oxygen species (ROS) scavenging activity of urolithin A (UA). The cells were pretreated with UA for 6 h, and then treated with 300 μM H_2O_2 for 18 h. The results are expressed as mean ± SD. Different letters indicate a significant difference according to analysis of variance ($P < 0.05$).

However, pretreatment with UA significantly diminished the increase in intracellular ROS production (Fig. 2).

UA inhibits H_2O_2-induced apoptosis

To demonstrate the anti-apoptotic effects of UA, we confirmed the protein expressions of Bcl2 and Bax via Western blotting analyses. In the 300 μM H_2O_2 treatment group, the Bax/Bcl2 ratio increased approximately three-fold compared to the control group. However, UA pretreatment resulted in a significant decrease in the Bax/Bcl2 ratio, particularly at UA concentrations of 2.5 and 5 μM, compared to the H_2O_2-treated group (Fig. 3A).

In addition, Hoechst 33342 staining showed DNA condensation and nuclear fragmentation after H_2O_2 treatment. However, these apoptotic characteristics were inhibited by pretreatment with UA (Fig. 3B). Taken together, the results imply that UA pretreatment inhibited H_2O_2-induced apoptosis.

UA prevents apoptotic cell death by suppressing the expression of mitochondrial-related apoptosis proteins

Next, we investigated the protein expression of the mitochondrial-related apoptosis pathway in H_2O_2-induced SK-N-MC cells in the presence or absence of UA. As shown in Fig. 4, H_2O_2 increased the expressions of cytochrome c, cleaved caspase-9, cleaved caspase-3, and cleaved PARP. However, in the UA pretreatment group, the expressions of these mitochondrial-related apoptosis proteins were suppressed, demonstrating that UA attenuates apoptotic cell death by its anti-apoptotic properties against H_2O_2-induced apoptosis in SK-N-MC cells.

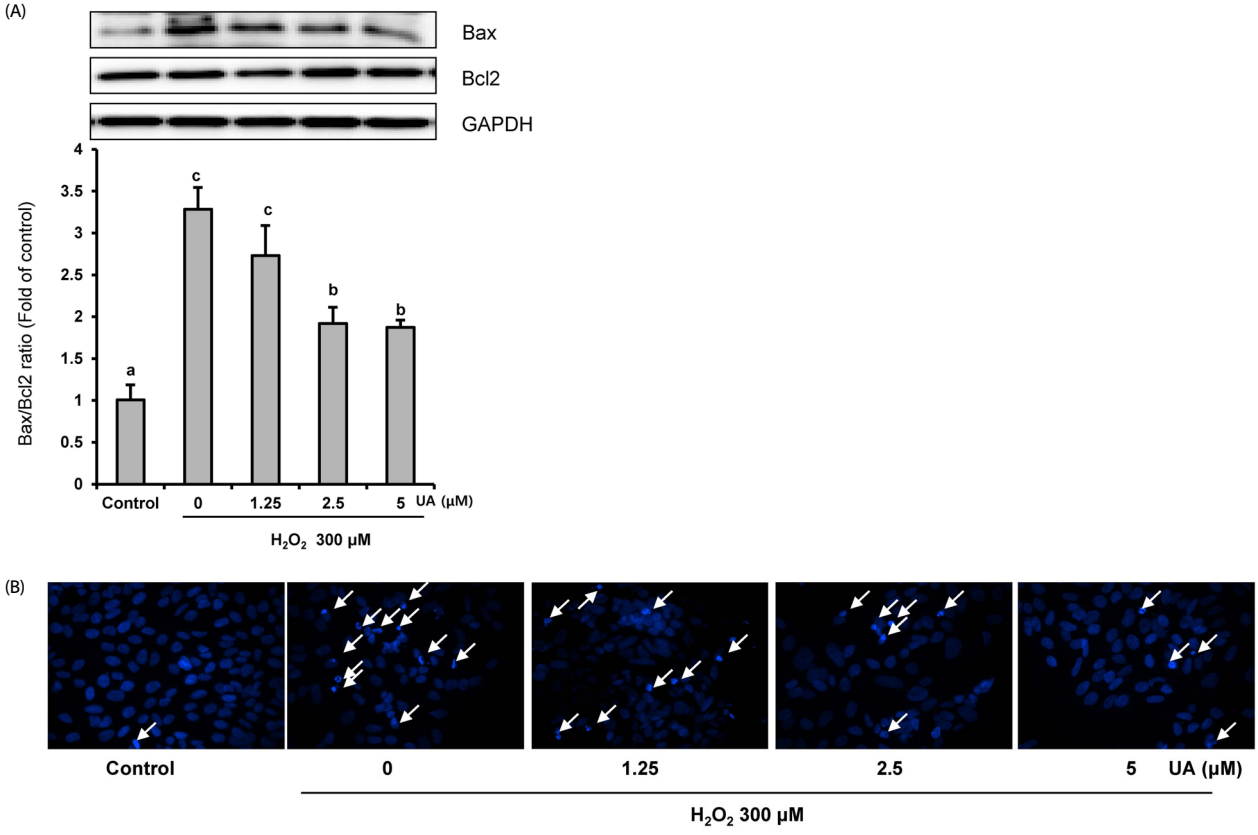

Fig. 3. Urolithin A (UA) inhibits H_2O_2-induced apoptosis. Cells were pretreated with UA for 6 h, and then treated with 300 μM H_2O_2 for 18 h. (A) The expression of Bax and Bcl2 were analyzed by Western blotting and normalized to the levels of GAPDH. The results are expressed as mean ± SD. Different letters indicate a significant difference according to analysis of variance ($P < 0.05$). (B) Morphological changes of nuclear chromatin by Hoechst 33342 staining were observed using the fluorescence microscope. Hoechst dye stained both fragmented and condensed nuclei (arrowheads)

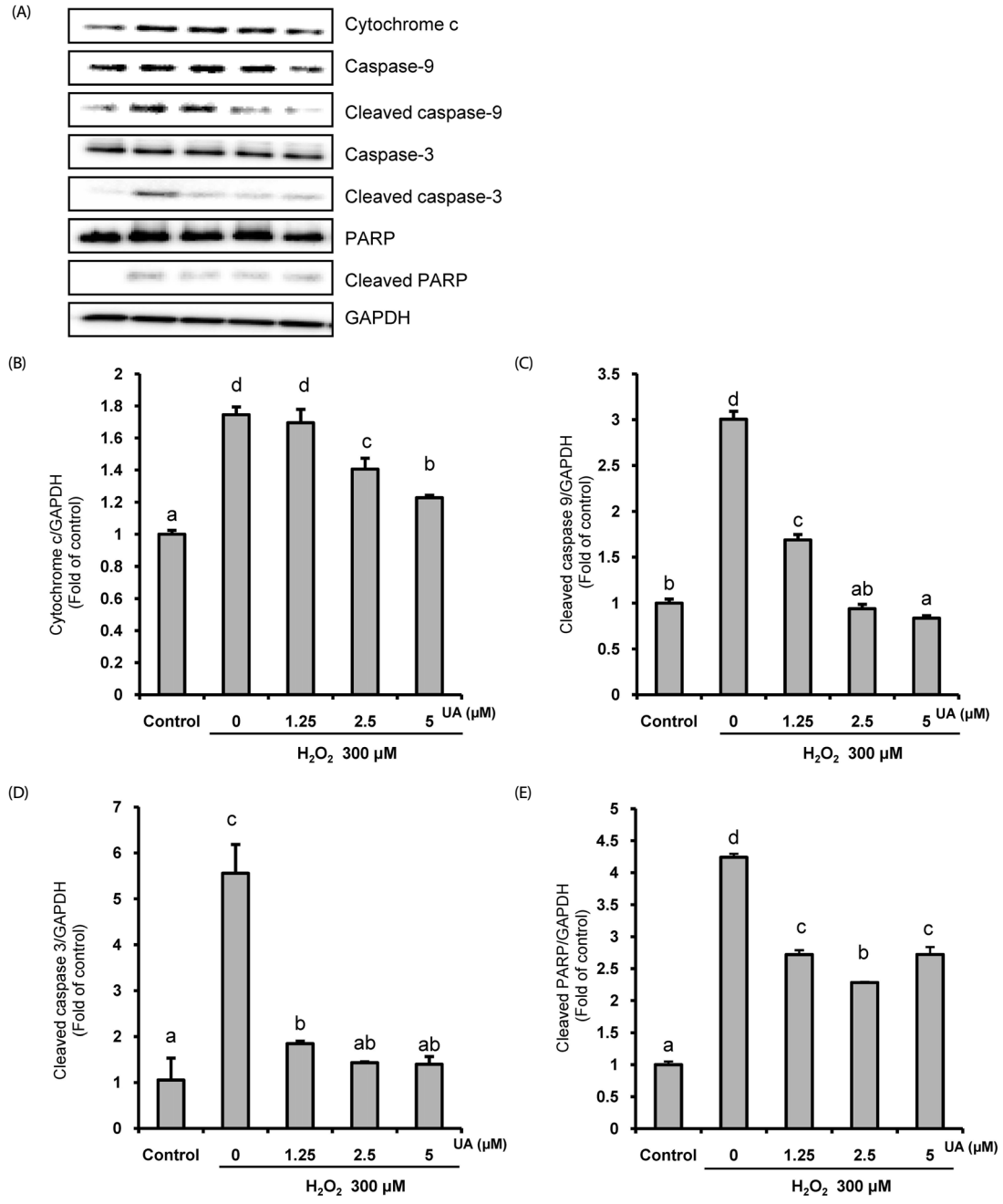

Fig. 4. Effects of urolithin A (UA) on the mitochondria-related apoptosis pathway. The cells were pretreated with UA for 6 h, then treated with 300 μM H_2O_2 for 18 h. (A) The protein expression by Western blotting. (B-E) Quantitative analysis of the bar graphs showed the densities of the protein bands; (B) cytochrome c, (C) cleaved caspase-9, (D) cleaved caspase-3, and (E) cleaved PARP. The normalization of cytochrome c, cleaved caspase-9, cleaved caspase-3, and cleaved PARP used GAPDH. The results are expressed as mean ± SD. Different letters indicate a significant difference according to analysis of variance ($P < 0.05$).

UA has protective effects by modulating the p38 MAPK pathway.

The mitogen-activated protein kinase (MAPK) signal pathway, including c-Jun N-terminal kinase (JNK), extracellular signal-regulated kinase (ERK), and p38 was activated by ROS. We investigated whether UA regulated the MAPK signal pathway in SK-N-MC cells. As shown in Fig. 5, pretreatment with UA significantly reduced the expression of p-p38 induced by H_2O_2. However, the effects on the expressions of p-JNK and p-ERK were not significant (data not shown).

To further confirm the action of UA on the p-p38 MAPK pathway, changes in cell viability were measured by treating cells with a p38 MAPK inhibitor (SD203580) (Fig. 5B). The cell viability decreased to 65.8 ± 1.5% when treated with H_2O_2, but was significantly increased by treatment with p38 MAPK inhibitor and UA (77.9 ± 3.6% and 78.6 ± 1.2%, respectively). In addition, the cell viability was further increased to 83.7 ± 0.6%

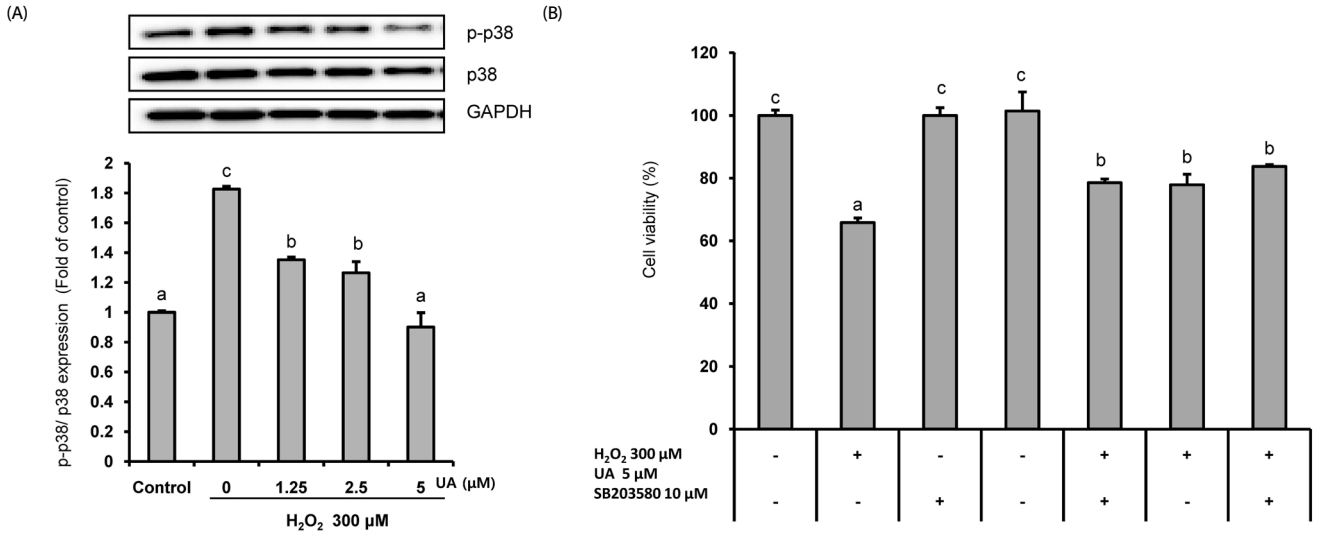

Fig. 5. Urolithin A (UA) attenuated H_2O_2-induced SK-N-MC cell death by modulating the p38 MAPK signaling pathway. (A) The cells pretreated with UA for 6 h, and then treated with 300 μM H_2O_2 for 18 h. The protein levels of phosphorylated p38, total p38, and GAPDH were determined by Western blotting and normalized to the levels of GAPDH. (B) The cells were pretreated with SB206580 (p38 MAPK inhibitor) for 1 h, treated 5 μM UA for 6 h, and then treated with 300 μM H_2O_2 for 18 h. The cell viability was measured using the CCK-8 assay. The results are expressed as mean ± SD. Different letters indicate a significant difference according to analysis of variance (P< 0.05).

in the group pretreated with p38 MAPK inhibitor and UA. Together, the results indicate that UA treatment suppresses H_2O_2-induced neuronal cell death by modulating the p38 MAPK pathway.

DISCUSSION

Polyphenols are converted into small molecular metabolites by gut microbiota. The converted metabolites have the advantages of excellent body utilization and high BBB permeability, compared to polyphenols [13,24]. Therefore, metabolites derived from gut microbes are expected to be effective protective agents for the prevention and treatment of brain-related diseases. In this study, we hypothesized that UA, a representative polyphenol metabolite, may have neuroprotective effects by inhibiting cell death induced by oxidative stress.

ETs, which are abundant in pomegranates, berries, and nuts, are hydrolyzed into EA in the body after ingestion as a kind of water-soluble tannin, and hydrolyzed EA is metabolized by Uros [17,24,25]. ETs and EA have anti-inflammatory, antioxidant, and anti-cancer effects [26,27], but dietary EA has low bioavailability, due to its low solubility in the stomach and limited absorption in the intestine [14,28-30]. González-Sarrías *et al*. [31] reported that EA concentrations in the plasma or tissues do not exceed 100 nM, even after oral ingestion of pure EA at high concentrations. However, when EA is converted into UA, the uptake in the intestinal villi increases and is maintained at a high level in the plasma, allowing circulation to the target tissue through the blood [11,28,32]. Cerda *et al*. [33] detected UA levels in plasma of up to 14-40 μM after administering pomegranate juice to healthy people, and there was no apparent toxicity. Vicinanza *et al*. [34] also reported high concentrations of UA in the target tissues of animal models after oral administration. Therefore, after intestinal absorption, UA has high bioavailability because can reach concentrations in the bloodstream that can exert effects *in vivo*. Moreover, UAs circulating through the blood can penetrate the BBB. The BBB is a interface that limits and regulates molecular exchanges between the blood and the neuronal tissue or its fluid spaces, having a crucial role in providing nutrients and controlling the access of compounds to the brain [35,36]. Although high-molecular-weight polyphenols such as ETs is not able to cross the BBB, UA conversed into low-molecular-weight metabolites has high permeability on the BBB [28,37]. UA is the major form found in humans [17,32]. It has antioxidant [38], anti-inflammatory [18], and anti-cancer [13,29,30,32] effects, attenuates endothelial dysfunction [39], and inhibits fat accumulation [17]. However, few studies on the action of UA in relation to the pathogenesis of NDs due to oxidative stress have been conducted. We expected that UA would has potential a therapeutic effect on the NDs by reducing loss of brain tissue through protection of neuronal cells. Therefore, we investigated the neuroprotective effects of UA on oxidative stress.

UA pretreatment increased the cell viability reduced by H_2O_2 in SK-N-MC cells (Fig. 1). It also decreased the increased intracellular ROS production (Fig. 2). According to many previous *in vitro* studies, hydrogen peroxide (H_2O_2) had toxic effects on various cells, including neurons, by causing oxidative damage to nucleic acids, proteins, and cell membrane lipids [7,10,40]. In our study, UA protected cells against H_2O_2 toxicity and inhibited the induction of oxidative damage by ROS. UA exhibits antioxidative effects through removal of free radicals [41] and inhibition of pro-oxidative enzymes such as heme-peroxidase [38]. Therefore, we conclude that the antioxidant activity of UA protected SK-N-MC neuronal cells from oxidative damage by H_2O_2. Tang *et al*. [18] also reported that when hypoxia/reoxygenation (H/R) injury was induced in primary cultured neonatal rat cardiomocytes, decreased cell viability and increased accumulation of intracellular ROS were attenuated by pretreatment with 10 μM UA. Although there have been several

reports that high concentrations (> 50 μM) of UA have anti-proliferative effects in various cancer cell lines [13,17], a study using SH-SY5Y human neuroblastoma cells reported that pretreatment with 10 μM UA inhibited the reduction of cell viability by H_2O_2 [11]. Moreover, our results demonstrate that low concentrations (≤ 5 μM) of UA may alleviate inhibition of cell growth by oxidative stress in SK-N-MC human neuroblastoma cells. Thus, we investigated the mechanism of the neuroprotective effects of UA based on the results of Figs. 1 and 2.

The first mechanism of UA protection against neuronal apoptosis is inhibition of apoptosis through regulation of mitochondrial-related apoptosis pathways. Mitochondria play important roles in intracellular energy metabolism. Oxidative stress induce alteration in mitochondrial protein, lipids, and DNA. Structural damage of the mitochondria results in defects in mitochondrial function, that are connected apoptosis and caspase activation which in turn leads to the damage to nerve cell. Therefore, mitochondrial dysfunction has a crucial role in the pathophysiology of NDs [25,42]. ROS-induced damage to mitochondrial membranes opens mitochondrial permeability transition pores (MPTPs), which induces release of mitochondrial cytochrome c. This activates caspase-9, which in turn triggers activation of caspase-3, leading to DNA damage, which impairs mitochondrial function [5,6]. During this process, members of the Bcl-2 family play important regulatory roles in the mitochondrial-related apoptosis pathway. Bax, a proapoptotic member, promotes apoptosis by accelerating the opening of MPTPs and inhibiting apoptosis via the anti-apoptotic Bcl-2 pathway [43]. In the present study, we confirmed increases in the Bax/Bcl-2 ratio, apoptotic nuclei, and expressions of cytochrome c, cleaved caspase-9, cleaved caspase-3, and cleaved PARP after H_2O_2 treatment. However, all of these apoptotic cell signals induced by H_2O_2 were significantly reduced by pretreatment with 2.5 and 5 μM UA (Figs. 3 and 4). Thus, UA inhibited apoptosis of SK-N-MC cells by inhibiting the mitochondrial-related apoptosis pathway. Tang *et al*. [18] reported that UA inhibits apoptosis of neonatal rat cardiomyocytes during hypoxia/reoxygenation (H/R) injury via the PI3K/Akt pathway. In addition, there have been many reports on the preventive competence and mechanism of EA, a metabolite precursor of UA. Firdaus *et al*. [44] reported that EA ameliorates mitochondrial dysfunction by reducing mitochondrial membrane potential and cytochrome c release against AS_2O_3-induced toxicity in SH-SY5Y human neuroblastoma cells. Chen *et al*. [45] reported that EA suppresses apoptosis by regulating the expressions of Bax, Bcl-2, and caspase-3 in the livers and brains of rats treated with D-galactose. In addition, Baluchnejadmojarad *et al*. [46] showed that EA has a protective effect via Nrf2/HO-1 signaling in a rat model of PD. These studies support our results that UA inhibits apoptosis. Therefore, we suggest that UA, which can pass through the BBB, may have a therapeutic effect on neurodegenerative diseases by ameliorating mitochondrial dysfunction of neuronal cells due to oxidative stress.

A second mechanism for the neuroprotective effects of UA involves modulation of the p38 MAPK pathway. MAPK pathways play an important role in cell proliferation, differentiation, and apoptosis regulation [47], and they are activated by various cell stress stimuli such as oxidative stress and endoplasmic reticulum stress [48]. The MAPK signaling pathway is involved in the pathogenesis of various diseases, including cancer and NDs. In the case of AD, activation of the MAPK pathway leads to neuronal apoptosis, β-secretase activity, γ-secretase activity, and tau phosphorylation [49]. In our study, pretreatment with UA significantly reduced expression of phosphorylated p38 MAPK (Fig. 5A). It also mitigated cell viability reduced by H_2O_2 via inhibition of the p38 MAPK signaling pathway (Fig. 5B). Although we did not confirm the effects of UA on phosphorylated ERK and the JNK pathway (data not shown), our results clearly indicate that UA protects cells from cytotoxicity by inhibiting activation of the p38 MAPK pathway. Chen *et al*. [50] showed that oral administration of EA induced downregulation of the JNK, p38 pathway and inflammatory mediators such as TNF-α, IL-1α, IL-1β, and COX-2 in induced hypoxic-ischemic brain-injury animal models. González-Sarrías *et al*. [51] reported that ≥ 10 μM EA and UA mitigated the inflammatory state in human colonic fibroblasts that induced inflammation by IL-1β via inhibiting the activation of NF-kB and the p38 MAPK pathway. In addition, Komatu *et al*. [16] reported that pretreatment with 40 μM UA inhibited the phosphorylation of p38 and JNK in inflammation-induced RAW264 macrophages induced by lipopolysaccharide, and also the formation of various proinflammatory mediators such as TNF-a, IL-6, and NO. In addition, p38 MAPK inhibitors are potential drug treatments for AD, and play an important role in the production of $A\beta_{42}$-induced proinflammatory cytokines [52]. Therefore, we propose that UA inhibits the p38 MAPK pathway, which is an important mechanism for protecting neuronal cells and brain tissue through anti-apoptosis and anti-inflammatory effects.

In conclusion, UA inhibited apoptotic cell death involving oxidative stress by decreasing intracellular ROS production, inhibiting the mitochondrial-related apoptosis pathway, and modulating the p-38 MAPK pathway. Taken together, our results indicate that UA protects against H_2O_2-induced growth inhibition and apoptosis induction in SK-N-MC cells. Thus, we suggest that it could be a useful neuroprotective agent against oxidative stress-related brain diseases. Future studies should examine the metabolic processes of UA and its protective effects on brain tissue in animal models of AD and PD.

CONFLICT OF INTEREST

The authors declare no conflict of interest.

ORCID

Kkot Byeol Kim: https://orcid.org/0000-0002-0407-191X
Seonah Lee: https://orcid.org/0000-0003-2136-2601
Jung Hee Kim: https://orcid.org/0000-0003-2156-1993

REFERENCES

1. Liguori I, Russo G, Curcio F, Bulli G, Aran L, Della-Morte D, Gargiulo G, Testa G, Cacciatore F, Bonaduce D, Abete P. Oxidative stress, aging, and diseases. Clin Interv Aging 2018;13:757-72.
2. Chung MJ, Lee S, Park YI, Lee J, Kwon KH. Neuroprotective effects of phytosterols and flavonoids from Cirsium setidens and Aster

scaber in human brain neuroblastoma SK-N-SH cells. Life Sci 2016;148:173-82.
3. Kim S, Chin YW, Cho J. Protection of cultured cortical neurons by luteolin against oxidative damage through inhibition of apoptosis and induction of heme oxygenase-1. Biol Pharm Bull 2017;40:256-65.
4. Moslehi M, Yazdanparast R. SK-N-MC cell death occurs by distinct molecular mechanisms in response to hydrogen peroxide and superoxide anions: involvements of JAK2-STAT3, JNK, and p38 MAP kinases pathways. Cell Biochem Biophys 2013;66:817-29.
5. Tian X, Gao L, An L, Jiang X, Bai J, Huang J, Meng W, Zhao Q. Pretreatment of MQA, a caffeoylquinic acid derivative compound, protects against H_2O_2-induced oxidative stress in SH-SY5Y cells. Neurol Res 2016;38:1079-87.
6. Tian X, Sui S, Huang J, Bai JP, Ren TS, Zhao QC. Neuroprotective effects of *Arctium lappa* L. roots against glutamate-induced oxidative stress by inhibiting phosphorylation of p38, JNK and ERK 1/2 MAPKs in PC12 cells. Environ Toxicol Pharmacol 2014;38:189-98.
7. Gay NH, Phopin K, Suwanjang W, Songtawee N, Ruankham W, Wongchitrat P, Prachayasittikul S, Prachayasittikul V. Neuroprotective effects of phenolic and carboxylic acids on oxidative stress-induced toxicity in human neuroblastoma SH-SY5Y cells. Neurochem Res 2018;43:619-36.
8. Nataraj J, Manivasagam T, Justin Thenmozhi A, Essa MM. Neuroprotective effect of asiatic acid on rotenone-induced mitochondrial dysfunction and oxidative stress-mediated apoptosis in differentiated SH-SYS5Y cells. Nutr Neurosci 2017;20:351-9.
9. Chen C, Cao J, Ma X, Wang X, Chen Q, Yan S, Zhao N, Geng Z, Wang Z. Neuroprotection by polynitrogen manganese complexes: regulation of reactive oxygen species-related pathways. Sci Rep 2016;6:20853.
10. Park HR, Lee H, Park H, Jeon JW, Cho WK, Ma JY. Neuroprotective effects of *Liriope platyphylla* extract against hydrogen peroxide-induced cytotoxicity in human neuroblastoma SH-SY5Y cells. BMC Complement Altern Med 2015;15:171.
11. DaSilva NA, Nahar PP, Ma H, Eid A, Wei Z, Meschwitz S, Zawia NH, Slitt AL, Seeram NP. Pomegranate ellagitannin-gut microbial-derived metabolites, urolithins, inhibit neuroinflammation *in vitro*. Nutr Neurosci 2019;22:185-95.
12. Cardona F, Andrés-Lacueva C, Tulipani S, Tinahones FJ, Queipo-Ortuño MI. Benefits of polyphenols on gut microbiota and implications in human health. J Nutr Biochem 2013;24:1415-22.
13. Wang Y, Qiu Z, Zhou B, Liu C, Ruan J, Yan Q, Liao J, Zhu F. *In vitro* antiproliferative and antioxidant effects of urolithin A, the colonic metabolite of ellagic acid, on hepatocellular carcinomas HepG2 cells. Toxicol In Vitro 2015;29:1107-15.
14. Esteban-Fernández A, Rendeiro C, Spencer JP, Del Coso DG, de Llano MD, Bartolomé B, Moreno-Arribas MV. Neuroprotective effects of selected microbial-derived phenolic metabolites and aroma compounds from wine in human SH-SY5Y neuroblastoma cells and their putative mechanisms of action. Front Nutr 2017;4:3.
15. Liu QS, Li SR, Li K, Li X, Yin X, Pang Z. Ellagic acid improves endogenous neural stem cells proliferation and neurorestoration through Wnt/β-catenin signaling *in vivo* and *in vitro*. Mol Nutr Food Res 2017;61:1600587.
16. Komatsu W, Kishi H, Yagasaki K, Ohhira S. Urolithin A attenuates pro-inflammatory mediator production by suppressing PI3-K/Akt/NF-κB and JNK/AP-1 signaling pathways in lipopolysaccharide-stimulated RAW264 macrophages: possible involvement of NADPH oxidase-derived reactive oxygen species. Eur J Pharmacol 2018;833:411-24.
17. Kang I, Kim Y, Tomás-Barberán FA, Espín JC, Chung S. Urolithin A, C, and D, but not iso-urolithin A and urolithin B, attenuate triglyceride accumulation in human cultures of adipocytes and hepatocytes. Mol Nutr Food Res 2016;60:1129-38.
18. Tang L, Mo Y, Li Y, Zhong Y, He S, Zhang Y, Tang Y, Fu S, Wang X, Chen A. Urolithin A alleviates myocardial ischemia/reperfusion injury via PI3K/Akt pathway. Biochem Biophys Res Commun 2017;486:774-80.
19. Wang S, Xia B, Qiao Z, Duan L, Wang G, Meng W, Liu Z, Wang Y, Zhang M. Tetramethylpyrazine attenuated bupivacaine-induced neurotoxicity in SH-SY5Y cells through regulating apoptosis, autophagy and oxidative damage. Drug Des Devel Ther 2019;13:1187-96.
20. Tu G, Zhang YF, Wei W, Li L, Zhang Y, Yang J, Xing Y. Allicin attenuates H_2 O_2 -induced cytotoxicity in retinal pigmented epithelial cells by regulating the levels of reactive oxygen species. Mol Med Rep 2016;13:2320-6.
21. Kim KB, Lee S, Kang I, Kim JH. *Momordica charantia* ethanol extract attenuates H_2O_2-induced cell death by its antioxidant and anti-apoptotic properties in human neuroblastoma SK-N-MC cells. Nutrients 2018;10:1368.
22. Lee KH, Lee SJ, Lee HJ, Choi GE, Jung YH, Kim DI, Gabr AA, Ryu JM, Han HJ. Amyloid β1-42 (Aβ1-42) induces the CDK2- mediated phosphorylation of tau through the activation of the mTORC1 signaling pathway while promoting neuronal cell death. Front Mol Neurosci 2017;10:229.
23. Lee HJ, Ryu JM, Jung YH, Lee SJ, Kim JY, Lee SH, Hwang IK, Seong JK, Han HJ. High glucose upregulates BACE1-mediated Aβ production through ROS-dependent HIF-1α and LXRα/ABCA1-regulated lipid raft reorganization in SK-N-MC cells. Sci Rep 2016;6:36746.
24. Gerhauser C. Impact of dietary gut microbial metabolites on the epigenome. Philos Trans R Soc Lond B Biol Sci 2018;373:20170359.
25. Nicolson GL. Mitochondrial dysfunction and chronic disease: treatment with natural supplements. Integr Med (Encinitas) 2014;13:35-43.
26. Heber D. Multitargeted therapy of cancer by ellagitannins. Cancer Lett 2008;269:262-8.
27. Espín JC, Larrosa M, García-Conesa MT, Tomás-Barberán F. Biological significance of urolithins, the gut microbial ellagic acid-derived metabolites: the evidence so far. Evid Based Complement Alternat Med 2013;2013:270418.
28. Kojadinovic M, Arsic A, Petovic-Oggiano G, Gavrovic-Jankulovic M, Glibetic M, Popovic M. Effect of urolithins on oxidative stress of colorectal adenocarcinomacells-Caco-2. Int J Food Sci Nutr 2017;68:952-9.
29. Zhao W, Shi F, Guo Z, Zhao J, Song X, Yang H. Metabolite of ellagitannins, urolithin A induces autophagy and inhibits metastasis in human sw620 colorectal cancer cells. Mol Carcinog 2018;57:193-200.
30. Liberal J, Carmo A, Gomes C, Cruz MT, Batista MT. Urolithins impair cell proliferation, arrest the cell cycle and induce apoptosis in UMUC3 bladder cancer cells. Invest New Drugs 2017;35:671-81.
31. González-Sarrías A, García-Villalba R, Núñez-Sánchez MA, Tomé-Carneiro J, Zafrilla P, Mulero J, Tomás-Barberán FA, Espín JC. Identifying the limits for ellagic acid bioavailability: a crossover pharmacokinetic study in healthy volunteers after consumption of pomegranate extracts. J Funct Foods 2015;19:225-35.

32. Nuñez-Sánchez MA, García-Villalba R, Monedero-Saiz T, García-Talavera NV, Gómez-Sánchez MB, Sánchez-Álvarez C, García-Albert AM, Rodríguez-Gil FJ, Ruiz-Marín M, Pastor-Quirante FA, Martínez-Díaz F, Yáñez-Gascón MJ, González-Sarrías A, Tomás-Barberán FA, Espín JC. Targeted metabolic profiling of pomegranate polyphenols and urolithins in plasma, urine and colon tissues from colorectal cancer patients. Mol Nutr Food Res 2014;58:1199-211.
33. Cerdá B, Espín JC, Parra S, Martínez P, Tomás-Barberán FA. The potent *in vitro* antioxidant ellagitannins from pomegranate juice are metabolised into bioavailable but poor antioxidant hydroxy-6H-dibenzopyran-6-one derivatives by the colonic microflora of healthy humans. Eur J Nutr 2004;43:205-20.
34. Vicinanza R, Zhang Y, Henning SM, Heber D. Pomegranate juice metabolites, ellagic acid and urolithin A, synergistically inhibit androgen-independent prostate cancer cell growth via distinct effects on cell cycle control and apoptosis. Evid Based Complement Alternat Med 2013;2013:247504.
35. Kujawska M, Jodynis-Liebert J. Polyphenols in Parkinson's disease: a systematic review of *in vivo* studies. Nutrients 2018;10:E642.
36. Figueira I, Garcia G, Pimpão RC, Terrasso AP, Costa I, Almeida AF, Tavares L, Pais TF, Pinto P, Ventura MR, Filipe A, McDougall GJ, Stewart D, Kim KS, Palmela I, Brites D, Brito MA, Brito C, Santos CN. Polyphenols journey through blood-brain barrier towards neuronal protection. Sci Rep 2017;7:11456.
37. Gasperotti M, Passamonti S, Tramer F, Masuero D, Guella G, Mattivi F, Vrhovsek U. Fate of microbial metabolites of dietary polyphenols in rats: is the brain their target destination? ACS Chem Neurosci 2015;6:1341-52.
38. Saha P, Yeoh BS, Singh R, Chandrasekar B, Vemula PK, Haribabu B, Vijay-Kumar M, Jala VR. Gut microbiota conversion of dietary ellagic acid into bioactive phytoceutical urolithin A inhibits heme peroxidases. PLoS One 2016;11:e0156811.
39. Ryu D, Mouchiroud L, Andreux PA, Katsyuba E, Moullan N, Nicolet-Dit-Félix AA, Williams EG, Jha P, Lo Sasso G, Huzard D, Aebischer P, Sandi C, Rinsch C, Auwerx J. Urolithin A induces mitophagy and prolongs lifespan in *C. elegans* and increases muscle function in rodents. Nat Med 2016;22:879-88.
40. Choi DJ, Cho S, Seo JY, Lee HB, Park YI. Neuroprotective effects of the *Phellinus linteus* ethyl acetate extract against H_2O_2-induced apoptotic cell death of SK-N-MC cells. Nutr Res 2016;36:31-43.
41. Ishimoto H, Tai A, Yoshimura M, Amakura Y, Yoshida T, Hatano T, Ito H. Antioxidative properties of functional polyphenols and their metabolites assessed by an ORAC assay. Biosci Biotechnol Biochem 2012;76:395-9.
42. Sun S, Pan S, Miao A, Ling C, Pang S, Tang J, Chen D, Zhao C. Active extracts of black tea (*Camellia sinensis*) induce apoptosis of PC-3 prostate cancer cells via mitochondrial dysfunction. Oncol Rep 2013;30:763-72.
43. Chen XZ, Li JN, Zhang YQ, Cao ZY, Liu ZZ, Wang SQ, Liao LM, Du J. Fuzheng Qingjie recipe induces apoptosis in HepG2 cells via P38 MAPK activation and the mitochondria-dependent apoptotic pathway. Mol Med Rep 2014;9:2381-7.
44. Firdaus F, Zafeer MF, Waseem M, Anis E, Hossain MM, Afzal M. Ellagic acid mitigates arsenic-trioxide-induced mitochondrial dysfunction and cytotoxicity in SH-SY5Y cells. J Biochem Mol Toxicol 2018;32: e22024.
45. Chen P, Chen F, Zhou B. Antioxidative, anti-inflammatory and anti-apoptotic effects of ellagic acid in liver and brain of rats treated by D-galactose. Sci Rep 2018;8:1465.
46. Baluchnejadmojarad T, Rabiee N, Zabihnejad S, Roghani M. Ellagic acid exerts protective effect in intrastriatal 6-hydroxydopamine rat model of Parkinson's disease: possible involvement of ERβ /Nrf2/HO-1 signaling. Brain Res 2017;1662:23-30.
47. Chan PH. Role of oxidants in ischemic brain damage. Stroke 1996;27:1124-9.
48. Li J, O W, Li W, Jiang ZG, Ghanbari HA. Oxidative stress and neurodegenerative disorders. Int J Mol Sci 2014;14:24438-75.
49. Kim EK, Choi EJ. Pathological roles of MAPK signaling pathways in human diseases. Biochim Biophys Acta 2010;1802:396-405.
50. Chen SY, Zheng K, Wang Z. Neuroprotective effects of ellagic acid on neonatal hypoxic brain injury via inhibition of inflammatory mediators and down-regulation of JNK/p38 MAPK activation. Trop J Pharm Res 2016;15:241-51.
51. González-Sarrías A, Larrosa M, Tomás-Barberán FA, Dolara P, Espín JC. NF-κB-dependent anti-inflammatory activity of urolithins, gut microbiota ellagic acid-derived metabolites, in human colonic fibroblasts. Br J Nutr 2010;104:503-12.
52. Munoz L, Ralay Ranaivo H, Roy SM, Hu W, Craft JM, McNamara LK, Chico LW, Van Eldik LJ, Watterson DM. A novel p38 alpha MAPK inhibitor suppresses brain proinflammatory cytokine up-regulation and attenuates synaptic dysfunction and behavioral deficits in an Alzheimer's disease mouse model. J Neuroinflammation 2007;4:21.